

Contribution from the Departments of Chemistry, University of Maine at Orono, Orono, Maine 04469, and University of Bern, CH-3000 Bern, Switzerland

Single-Crystal Luminescence Study of the Layered Compound $\text{KAu}(\text{CN})_2$

N. Nagasundaram,[†] G. Roper,^{††} J. Biscoe,[†] J. W. Chai,[†] H. H. Patterson,^{*†} N. Blom,[§] and A. Ludi[§]

Received October 28, 1985

Single-crystal laser luminescence studies are reported for the layered compound potassium dicyanoaurate(I) in the temperature range 8–300 K. The room-temperature emission spectrum consists of a high-energy band at about 390 nm and a low-energy band at about 630 nm. At 8 K, the high-energy band has vibronic structure and the low-energy band has disappeared. Au–Au separations as a function of temperature were obtained by X-ray diffraction. A comparison of the emission band energies with Au–Au separation indicates that the high-energy emission band should be assigned to states arising from Au–Au overlaps in two dimensions. Polarization and lifetime results can be interpreted from simple molecular orbital considerations. The low-energy band in the single crystal and an additional emission band that appears for a powder are assigned to traps present in low concentrations.

Introduction

There has been much recent interest in two-dimensional layered compounds. The d^{10} Au(I) salts $\text{MAu}(\text{CN})_2$ ($M = \text{K}^+, \text{Cs}^+, \text{TI}^+$) have a crystal structure that consists of layers of $\text{Au}(\text{CN})_2^-$ linear ions alternating with layers of M^+ ions.^{1,2} When the cation is changed, the distance between gold atoms within a layer changes. For example, gold atoms are separated by 3.64 Å for the potassium salt at room temperature,¹ but for the tetrabutylammonium salt the nearest-neighbor Au separation is 8.8 Å.³ The optical absorption spectrum of the $\text{Au}(\text{CN})_2^-$ ion in aqueous solution shows charge-transfer absorption bands only at energies greater than 40 000 cm^{-1} while the K^+ , Cs^+ , and TI^+ salts of $\text{Au}(\text{CN})_2^-$ in the solid state have absorption bands shifted to lower energies by as much as 20 000 cm^{-1} .^{4,5} Therefore, a study of the K^+ , Cs^+ , and TI^+ salts of $\text{Au}(\text{CN})_2^-$ in the solid state provides an opportunity to study how the optical properties of layered compounds are related to the interactions between Au atoms within layers.

We have previously reported a low-temperature luminescence study of $\text{CsAu}(\text{CN})_2$, in which there are three inequivalent Au sites, unlike the case of the potassium salt, in which all the gold atom sites are equivalent.⁶ The luminescence bands in the Cs salt were assigned to emission from different Au(I) sites, and lifetime measurements vs. temperature (1–300 K) of the 430-nm band provided rate constants and relative energies for the development of a molecular orbital model with overlap of Au orbitals within the layers of the salt.

In this paper we report laser emission and X-ray measurements vs. temperature for d^{10} $\text{KAu}(\text{CN})_2$. These results allow us to determine the sensitivity of the emission energy to changes in Au–Au separation and to make a comparison with the one-dimensional d^8 tetracyanoplatinate(II) salts.

Experimental Methods

Single crystals of $\text{KAu}(\text{CN})_2$ were grown by slow evaporation of aqueous solutions. X-ray oscillation and Weissenberg patterns were used to determine the orientation of the hexagonal crystallographic axes. The variation with temperature of the nearest gold to gold distance was investigated by measuring the 600 interplanar spacing as a function of temperature using a single-crystal-diffractometer technique. For this purpose, a General Electric single-crystal diffractometer was modified so that the angular setting of the crystal, θ , and the angular setting of the counter, 2θ , could be independently controlled. To study the 600 interplanar spacings, the crystal was mounted with its c axis parallel to the diffractometer axis, and 2θ was set at the value calculated for the room-temperature value of d , and, with a wide receiving slit in place, θ was adjusted for maximum count. A narrow (0.05°) receiving slit was then installed and 2θ adjusted for maximum count. The process was then repeated for each temperature. To study the changes in the c -axis length, the crystal was mounted with the c axis perpendicular to the diffractometer axis and the spacings of the 0027 planes were measured. The 600 and 0027 reflections were chosen because they had adequate inten-

sities and reasonably high 2θ values, and there were no nearby reflections. A copper target tube was used.

The initial luminescence measurements were conducted with a Perkin-Elmer MPF-44A fluorescence spectrophotometer. Single-crystal luminescence spectra were measured by excitation at 337 nm using a Moletron UV Series 14 pulsed nitrogen laser with a pulse width of approximately 10 ns. An RCA 31034 photomultiplier tube and a McPherson Model 2051 monochromator with a Princeton Applied Research Model 124A lock-in amplifier comprised the detector system. Low temperatures were obtained by using an Air Products LT-3-110 Helitran. A Model 162 Princeton Applied Research Boxcar integrator was used for the lifetime measurements.⁷ Absorption measurements were done with a Cary 17D spectrophotometer.

Polarization measurements employed Polaroid HN P'B polarizers. The correction for the unequal transmission of the components of the polarized light by the emission monochromator grating was effected as follows. The emission beam emerging from the analyzer was passed through a second polarizer placed between the analyzer and the emission monochromator, with the second polarizer set at 45° to either position of the analyzer (0° and 90°). This arrangement ensured that for either position of the analyzer the beam incident on the emission monochromator had the same polarization ($I_1 \cos 45^\circ$ or $I_1 \sin 45^\circ$).

Results

Figure 1 shows the luminescence spectra for a $\text{KAu}(\text{CN})_2$ single crystal as a function of temperature (295, 140, 8 K) when excited with a pulsed nitrogen laser at 337 nm. The 295 K spectrum has a high-energy emission band at 390 nm and a low-energy band at 630 nm. As the crystal temperature is decreased, the low-energy band decreases in intensity and disappears below 120 K. At 8 K the high-energy band has vibronic structure. A $\text{KAu}(\text{CN})_2$ powder sample shows, in addition to the 390- and 630-nm bands, a third emission band at about 430 nm, which first appears at about 150 K and then increases in intensity as the temperature is lowered.

Both the high- and low-energy bands in the single-crystal emission spectra show a shift in position with a change in temperature. In contrast, the 430 nm powder emission band maximum is independent of temperature. In Figure 2 the high- and low-energy band maxima are plotted as a function of temperature. The data indicate that a temperature decrease from 300 to 78 K results in a decrease of the emission maximum energy of the

- (1) Rosenzweig, A.; Cromer, D. T. *Acta Crystallogr.* **1959**, *12*, 709.
- (2) (a) Blom, N.; Ludi, A.; Bürgi, H.-B.; Tichy, K. *Acta Crystallogr., Sect. C: Cryst. Struct. Commun.* **1984**, *C40*, 1767. (b) Blom, N.; Ludi, A.; Bürgi, H.-B. *Acta Crystallogr., Sect. C: Cryst. Struct. Commun.* **1984**, *C40*, 1770.
- (3) Mason, W. R. *J. Am. Chem. Soc.* **1976**, *98*, 5182.
- (4) Blom, N. Thesis, University of Bern, 1983.
- (5) Patterson, H. H.; Roper, G.; Biscoe, J.; Ludi, A.; Blom, N. *J. Lumin.* **1984**, *31/32*, 555.
- (6) Markert, J. T.; Blom, N.; Roper, G.; Perregaux, A. D.; Nagasundaram, N.; Corson, M. R.; Ludi, A.; Nagle, J. K.; Patterson, H. H. *Chem. Phys. Lett.* **1985**, *118*, 258.
- (7) Martin, M.; Krogh-Jespersen, M. B.; Hsu, M.; Tewksburg, J.; Laurent, M.; Viswanath, K.; Patterson, H. H. *Inorg. Chem.* **1983**, *22*, 647.

[†] University of Maine at Orono.

^{††} Permanent address: Department of Chemistry, Dickinson College, Carlisle, PA.

[§] University of Bern.

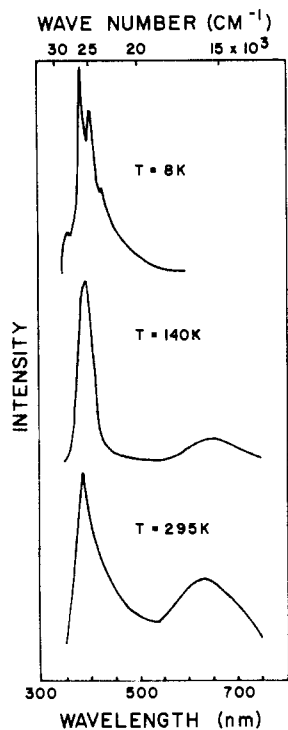


Figure 1. Laser-excited luminescence spectra of a single crystal of $\text{KAu}(\text{CN})_2$ at temperatures of 8, 140, and 295 K. Excitation wavelength: 337 nm.

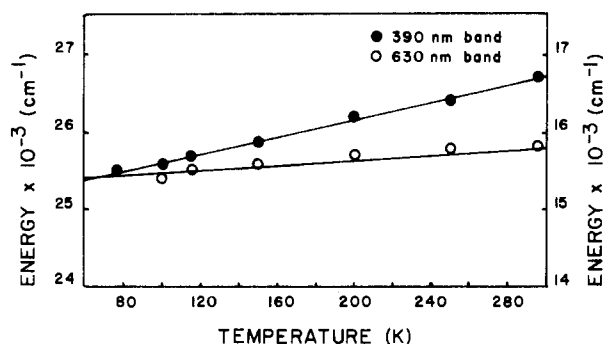


Figure 2. Temperature dependence of both the high- and low-energy emission maxima for a single $\text{KAu}(\text{CN})_2$ crystal with excitation wavelength equal to 337 nm.

high-energy band by 1100 cm^{-1} and of the low-energy band by 400 cm^{-1} .

X-ray measurements on $\text{KAu}(\text{CN})_2$ single crystals between room temperature and 78 K indicate the nearest-neighbor Au–Au separation decreases from 3.64 \AA at 278 K to 3.58 \AA at 78 K. Also, this temperature decrease results in an increase of 0.06 \AA in the separation between adjacent Au layers. In Figure 3 a plot is given of the fractional increase in the c axis and the fractional decrease in the a axis as the temperature is lowered from 278 to 78 K.

Polarized emission spectra were measured on a single $\text{KAu}(\text{CN})_2$ crystal oriented with the incident laser beam polarized parallel to the crystal c axis. Changing the polarization of the incident beam has no effect on the emission spectra. Figure 4 shows a plot of the polarization P of the high-energy emission band as a function of temperature. P is defined in eq 1,⁸ where I_{\parallel} and

$$P = (I_{\parallel} - I_{\perp}) / (I_{\parallel} + I_{\perp}) \quad (1)$$

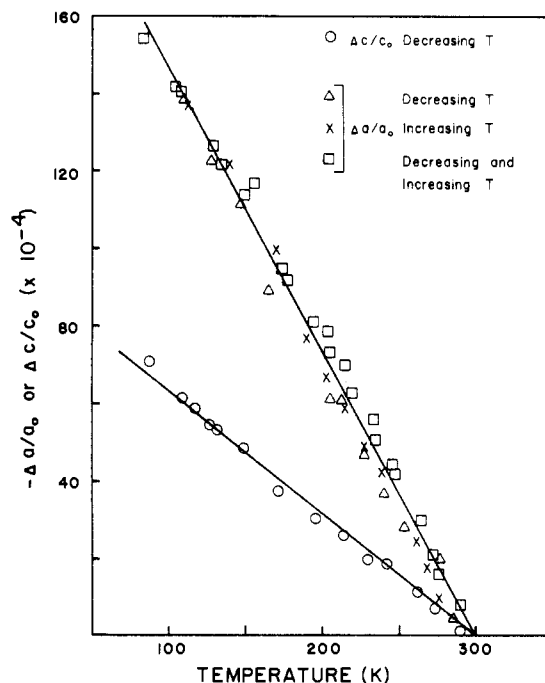


Figure 3. Fractional change of interplanar spacings as a function of temperature. a_0 ($=7.28 \text{ \AA}$) and c_0 ($=26.36 \text{ \AA}$) are the magnitudes of the unit cell vectors at room temperature. Physically a_0 is twice the in-plane Au–Au separation and c_0 , perpendicular to a_0 , represents 3 times the distance between the adjacent gold layers.

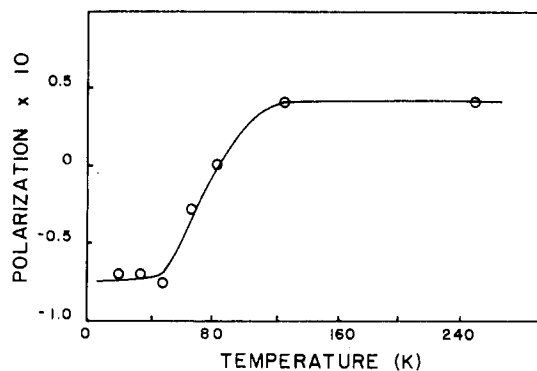


Figure 4. Polarization of the high-energy emission band of a $\text{KAu}(\text{CN})_2$ single crystal as a function of temperature. Polarization is defined in eq 1.

I_{\perp} are the intensities of the components of the emitted beam polarized parallel and perpendicular, respectively, to the c axis.

At 8 K a single $\text{KAu}(\text{CN})_2$ crystal shows structure for the high-energy emission band with peaks at 363, 388, 411, and 430 nm. Polarization measurements of the most intense peaks, at 388 and 411 nm, indicate that they both have the same polarization. Lifetime measurements of the four peaks at 8 K indicate that the time dependence of the emission intensities is best curve-fit by assuming emission occurs from two emitting states with approximately 20 and 140 ns values with relative intensities of 0.8 and 0.2, respectively. At 78 K the 390-nm band has only a single lifetime value of 200 ns, but at 300 K two lifetimes (120 and 7700 ns) are recorded. Also, at room temperature the 630-nm band has dual lifetimes of 1300 and 8500 ns.

Both the high-energy and low-energy emission bands for $\text{KAu}(\text{CN})_2$ have the same excitation maximum of 357 nm at room temperature. In Figure 5, in order to discuss energy transfer between the states responsible for the 390- and 630-nm emissions,

(8) Weber, G. *Fluorescence and Phosphorescence Analysis*; Hercules, D. M., Ed.; Wiley: New York, 1966; p 217.

(9) Jones, L. H. *J. Chem. Phys.* **1957**, *27*, 468.

(10) Laurent, M. P.; Patterson, H. H.; Pike, W.; Engstrom, H. *Inorg. Chem.* **1981**, *20*, 372.

(11) Day, P. J. *Am. Chem. Soc.* **1975**, *97*, 1588.

(12) Ellenson, W. D.; Viswanath, A. K.; Patterson, H. H. *Inorg. Chem.* **1981**, *20*, 780.

(13) Yersin, H.; Gliemann, G. *Ann. N.Y. Acad. Sci.* **1978**, *313*, 539.

(14) Yersin, H.; Gliemann, G.; Rossler, U. *Solid State Commun.* **1977**, *21*, 915.

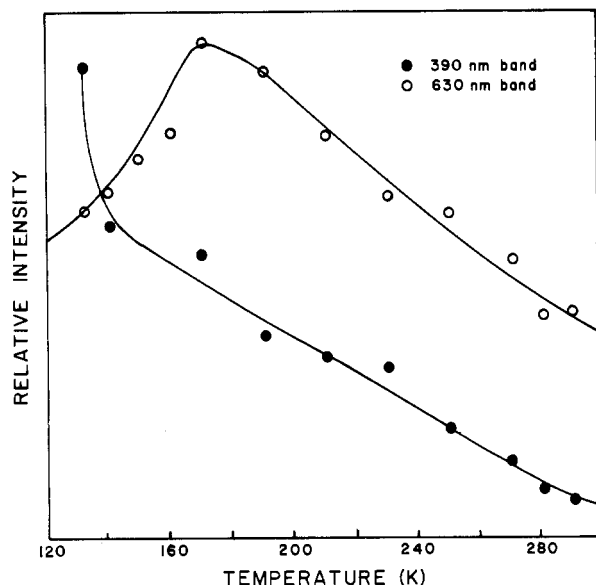


Figure 5. Intensities of the high- and low-energy emission bands vs. temperature for a $\text{KAu}(\text{CN})_2$ single crystal.

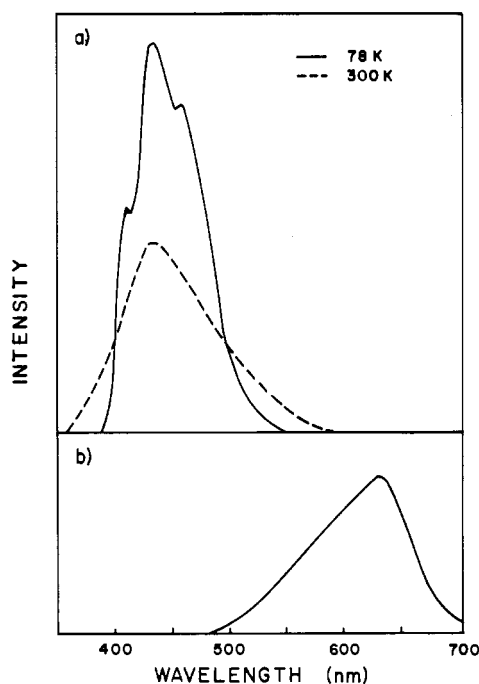


Figure 6. (a) Emission spectra at 300 and 78 K of $\text{KAu}(\text{CN})_2$ doped into a KCN single crystal. (b) Emission spectrum of AuCN at 300 K.

the intensities of these bands are plotted as a function of temperature.

Mixed crystals containing $\text{Au}(\text{CN})_2^-$ doped in a variety of hosts (KCl, KCN, NaCl, $\text{K}_2\text{Pt}(\text{CN})_6$) have been grown and the emission spectra recorded vs. temperature. In Figure 6 the emission spectra of $\text{Au}(\text{CN})_2^-$ doped in single crystals of KCN are shown for 300 and 78 K sample temperatures. At 300 K a single emission band at 420 nm is observed, which at 78 K appears as three peaks.

Discussion

Assignments for the 390-nm Emission Band. The space group of $\text{KAu}(\text{CN})_2$ is $R\bar{3}$ with rhombohedral lattice constants $a = 9.74 \text{ \AA}$ and $\alpha = 43.9^\circ$. The constants of the corresponding hexagonal triple cell are $a = 7.28 \text{ \AA}$ and $c = 26.36 \text{ \AA}$. The structure consists of layers of linear $\text{Au}(\text{CN})_2^-$ ions alternating with layers of K^+ ions. In a given layer the $\text{Au}(\text{CN})_2^-$ ions are, at room temperature, tilted 22° from the hexagonal c axis and the Au atoms lie in planes perpendicular to it. Every Au atom in a given layer has four nearest neighbors at 3.64 \AA in a rectangular environment.¹ The

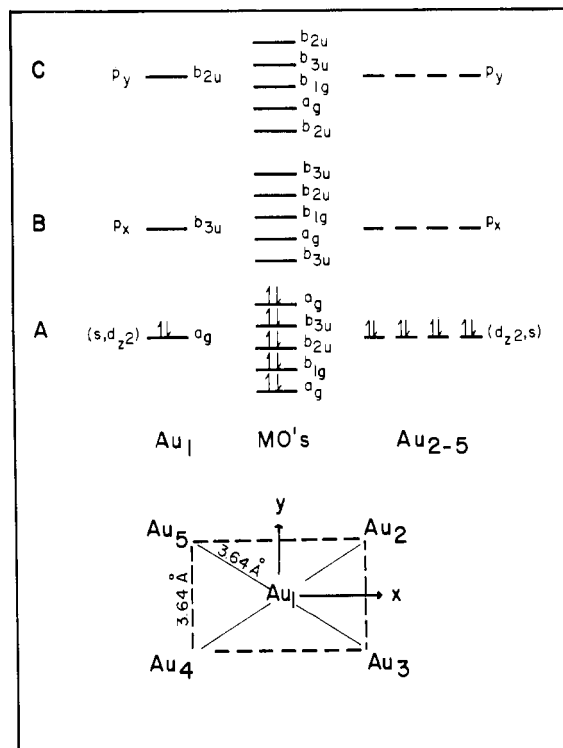


Figure 7. Interaction of the relevant atomic orbitals of neighboring Au atoms on a given layer to form molecular orbitals. The definition of the axes for a layer of gold atoms in $\text{KAu}(\text{CN})_2$ is also shown.

site symmetry with respect to the Au atoms alone within a given layer is D_{2h} , which is lowered to C_{2h} in the presence of CN^- ligands. The luminescence results for the high-energy band of $\text{KAu}(\text{CN})_2$ may be interpreted on the basis of the D_{2h} site symmetry considering nearest-neighbor Au-Au interactions.

The decrease of the high-energy-band emission energy with decreasing Au-Au distance within a layer suggests that the states involved in this transition correspond to metal orbitals with maximum overlap between nearest-neighbor gold atoms. The D_{2h} character table shows that σ Au-Au bonds may form with the $5d_{z^2}(a_g)$, $5d_{x^2-y^2}(a_g)$, $6s(a_g)$, $5d_{xy}(b_{1g})$, $6p_x(b_{3u})$, and $6p_y(b_{2u})$ orbitals, while π Au-Au bonds may form with $5d_{xz}(b_{2g})$, $5d_{yz}(b_{3g})$, and $6p_z(b_{1u})$ orbitals. The x and y axes are defined in Figure 7. There is strong evidence¹⁵ to suggest for isolated $\text{Au}(\text{CN})_2^-$ ions a σ HOMO of $6s$ and $5d_{z^2}$ composition, while the LUMO is largely $6p_x$ and $6p_y$ in character. Extended Hückel molecular orbital overlap calculations for the five $\text{Au}(\text{CN})_2^-$ units orientated as in Figure 7 indicate that for Au_1 interacting with Au_2 , Au_3 , Au_4 , and Au_5 the largest overlap integrals occur for the $6s$ orbitals. Group theory considerations of the overlap of the five $6s$ orbitals give the molecular orbitals shown in Figure 7, with the highest MO having a_g symmetry. Again, for Au_1 interacting with the neighboring Au_2 , Au_3 , Au_4 , and Au_5 atoms, the p_x orbitals are closer to each other than the p_y orbitals, and the Hückel MO overlap calculations indicate that the p_x orbitals overlap more strongly than the p_y orbitals. The interaction of the Au_1 p_x orbital with the neighboring Au p_x orbitals leads to the molecular orbitals shown in Figure 7 with the lowest energy molecular orbital having b_{3u} symmetry.

It is proposed that the high-energy emission band is due to the $a_g^2 \rightarrow a_g^1 b_{3u}^1$ electronic configuration change because the isolated ion HOMO and LUMO are mostly composed of $6s$ and $6p_x$, $6p_y$ atomic orbitals, respectively, which have the greatest overlap with neighboring $\text{Au}(\text{CN})_2^-$ ions for the D_{2h} symmetry case of Figure 7. Further, extended Hückel MO calculations of the five $\text{Au}(\text{CN})_2^-$ ions separated by a variable distance indicate that as the Au-Au separation is decreased, the energy difference between the HOMO and LUMO decreases.

For the $a_g^2 \rightarrow a_g^1 b_{3u}^1$ transition, the resulting excited states are a singlet ($^1B_{3u}$) and a triplet ($^3B_{3u}$), with the triplet state being lower in energy. Under the influence of spin-orbit interaction the $^3B_{3u}$ state splits into A_{2u}' (forbidden), B_{1u}' (z -polarized), and B_{2u}' (y -polarized). The primes are used to indicate the spin-orbit-split states.

The 8 K lifetime results for the 390-nm band, with both 20- and 200-ns lifetimes, suggest strongly that the emission occurs from both the $^1B_{3u} \rightarrow ^1A_{1g}$ (20 ns) and $^3B_{3u} \rightarrow ^1A_{1g}$ (200 ns) transitions. On the other hand, the 78 and 295 K lifetime values indicate that at these higher temperatures the intersystem radiationless process is quite effective, and thus, the $^3B_{3u} \rightarrow ^1A_{1g}$ type transition only is observed.

The average separation of the four peaks in the high-energy band at 8 K shown in Figure 1 is about 1400 cm^{-1} , with the separation greater for the higher energy portion of the peaks. Let us assume the observed luminescence structure is due to a progression in an $\text{Au}(\text{CN})_2^-$ ground electronic state vibrational mode with the energy of ν vibrational quanta given by

$$E(\nu) = \omega_e(\nu + 1/2) - \omega_e x_e(\nu + 1/2)^2 \quad (2)$$

Since $E(\nu + 1) - E(\nu) = \omega_e - 2\omega_e x_e(\nu + 1)$, a plot of $E(\nu + 1) - E(\nu)$ vs. $(\nu + 1)$ for $(\nu + 1) = 1, 2, \text{ and } 3$ gives a linear relation with $\omega_e = 2125 \pm 140 \text{ cm}^{-1}$ and $\omega_e x_e = 175 \pm 30 \text{ cm}^{-1}$. A room-temperature Raman study for $\text{KAu}(\text{CN})_2$ reported a value of 2164 cm^{-1} for the symmetric stretch CN mode energy.⁹ Anharmonicity constants of 23, 10, and 9 cm^{-1} for $\text{KAu}(\text{CN})_2$ at room temperature have been reported from vibrational combination peaks of mixed isotopic species.⁹ The ω_e values from the two measurements are in excellent agreement. The difference in the anharmonicity values are attributed to the facts that (1) the $\text{KAu}(\text{CN})_2$ luminescence measurement at 8 K may be reflective of greater anharmonicity than that at 300 K and (2) the luminescence spectrum consists of only 4 peaks for $\text{KAu}(\text{CN})_2$ in contrast to a similar analysis for Cs_2PtF_6 in which 13 peaks in the luminescence spectra were observed and excellent agreement was obtained with low-temperature Raman measurements.¹⁰ We conclude that the observed progression in the luminescence spectrum should be assigned to the symmetric stretch CN mode on the basis of the highest energy observed vibronic peak corresponding to a transition to the $\nu'' = 0$ level of the ground electronic state.

The relative energies of the $^3B_{3u}$ components (A_{1u}' , B_{1u}' , B_{2u}') can be determined from a plot of the polarization P vs. T given in Figure 4. The change in P at about 78 K from a (-) to a (+) value shows, from the definition of P in eq 1, that I_{\parallel} is greater than I_{\perp} ; this implies that B_{1u}' with \parallel polarization is becoming populated. Further, the fact that P remains constant above 200 K, and an additional 8- μs lifetime is observed, indicates that the newly populated state also has z polarization. A possible assignment for the 8- μs lifetime is emission from a B_{1u}' spin-orbit component arising from the p_x interaction (see Figure 7). Finally, we conclude from P and lifetime data vs. temperature that $E(B_{2u}') < E(B_{1u}') < E(A_{1u}')$.

Exciton Predictions. The optical properties of the one-dimensional d⁸ tetracyanoplatinate or -palladate salts are very similar to those of the $\text{Au}(\text{CN})_2^-$ salts.^{11,12} The $\text{Pt}(\text{CN})_4^{2-}$ ion in solution has no absorption bands below 35000 cm^{-1} , but the salts of the anion are brightly colored and show strong visible luminescence.⁹ Yersin et al. have demonstrated that the emission and reflectivity energies vary linearly as R^{-3} .^{13,14} Day has proposed that this behavior is characteristic of neutral Frenkel excitons.^{11,15} He has shown that the extrapolated energy of the transition at $R = \infty$ for the free ion is well within the expected energy.

In order to determine whether the high-energy emission band of $\text{KAu}(\text{CN})_2$ has exciton behavior, a plot of the emission energy E vs. R^{-3} has been made, where R is the in-plane Au-Au distance. A linear relation

$$E = E^\circ - aR^{-3} \quad (3)$$

was found, as shown in Figure 8, with the emission energy E° corresponding to an isolated ion. The calculated value of E° from

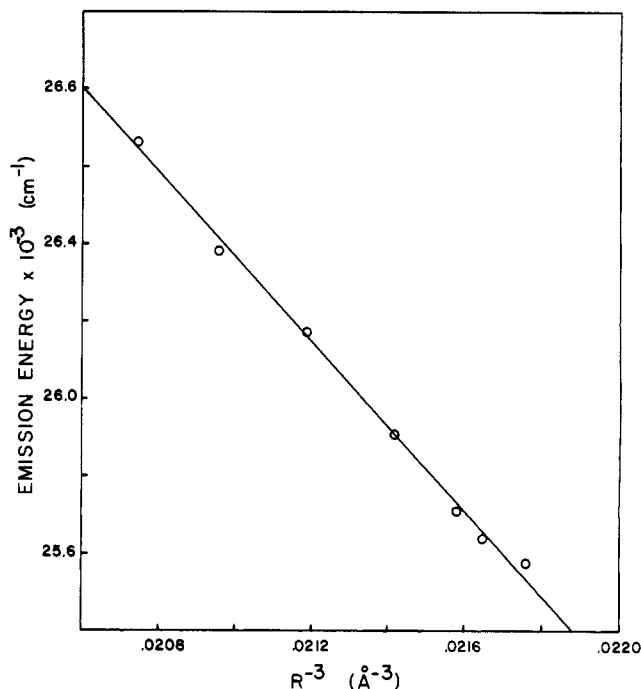
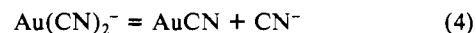


Figure 8. Emission energy of the high-energy band vs. R^{-3} indicating Au-Au interactions. R is the Au-Au distance within a given layer.

the plot is 43800 cm^{-1} , and a is equal to 8.21×10^5 . The experimental value of E° should correspond to a transition in the isolated ion similar to the emission transition assigned for $\text{KAu}(\text{CN})_2$. It has been reported to be about 42000 cm^{-1} for tetra-*n*-butylammonium dicyanoaurate(I), corresponding to the $\sigma_g(d_{z^2}, s)^2 \rightarrow \sigma_g(d_{z^2}, s)^1 \pi_u(p_x, p_y)^1$ configuration change.¹⁶ R for tetra-*n*-butylammonium dicyanoaurate(I) is 8.04 \AA so it can be considered as an isolated-ion case.³ The extrapolated and the literature experimental E° values are in reasonable agreement and suggest that the high-energy emitting states have Frenkel exciton behavior. The large shift in energy from the isolated ion to the $\text{KAu}(\text{CN})_2$ lattice of 18000 cm^{-1} indicates a very rapid transfer of excitation through the lattice.¹⁵

630-nm Emission Band. The 630-nm band has the same excitation spectrum as the 390-nm band. However, the 630-nm band is not polarized; that is P , as defined in eq 1, is equal to zero in the 120–300 K interval, where the peak is observed.

When $\text{KAu}(\text{CN})_2$ is doped into KCl crystals, the 630-nm peak appears in crystals with a small concentration of dopant. On the other hand, when $\text{KAu}(\text{CN})_2$ is doped into KCN crystals, for a range of concentrations the 630-nm band is always absent, as shown in Figure 6. It should be noted, however, that at 78 K the $\text{KAu}(\text{CN})_2$ -KCN spectrum has vibronic structure for the high-energy band similar to that for pure $\text{KAu}(\text{CN})_2$ at 8 K, shown in Figure 1, but shifted to lower energies by about 3000 cm^{-1} . This suggests that the low-energy band is possibly due to AuCN, where the $\text{Au}(\text{CN})_2^-$ has dissociated as in eq 4. The emission spectrum



of AuCN has a maximum at 630 nm, as shown in Figure 6; thus, the low-energy 630-nm band in $\text{KAu}(\text{CN})_2$ may be due to AuCN, existing not as a linear polymer but as an AuCN molecule. We believe that the reaction given in eq 4 occurs when light is incident on the sample because crystals that have been exposed to a N_2 laser for several hours sometimes show a yellow color similar to that of AuCN.

The $\text{KAu}(\text{CN})_2$ crystal structure consists of layers of gold perpendicular to the c axis. Within a layer the gold atoms are arranged in two-dimensional close-packing, with one out of four atoms missing.^{1,2} A K^+ ion is located above and below the missing

(16) Guenzburger, D.; Ellis, D. E. *Phys. Rev. B: Condens. Matter* **1980**, *22*, 4203.

Au atom site with a $K^+ - K^+$ distance of 8.22 Å. Since an AuCN molecule should be about 3.3 Å in length, the AuCN molecule could occupy the missing Au atom site and, because of its small size in comparison with the distance between neighbors, have a random orientation with a resulting zero P value. In contrast, the powder 430-nm emission band is assigned to emission of $Au(CN)_2^-$ occupying a surface site. This band does not shift in energy with changing temperature, but its relative intensity, in comparison with that of the 390-nm band, can be increased by heating the sample. This is similar to the behavior reported for surface states of metal oxide powder samples.^{17,18}

In order to characterize the dynamics of energy transfer between the states that give rise to the 390- and 630-nm bands, measurements have been made of the relative intensities of these bands as a function of temperature. As the temperature of a $KAu(CN)_2$ crystal increases from 80 to 300 K, the relative intensity of the 390-nm band decreases as shown in Figure 5. In contrast, as the temperature of a $KAu(CN)_2$ crystal is increased from 120 to 300 K, the 630-nm band intensity reaches a maximum between 160 and 180 K and then gradually decreases. Similar behavior has been reported for Er^{3+} -doped samples of $CsMnCl_3$ or $RbMnCl_3$.¹⁹

We interpret the initial increase in the 630-nm intensity from 120 to 160–180 K as arising from increased migration of the 390-nm excitation. A plot of $\log I_{630}$ vs. $1/T$ for ($80 < T < 180$ K) gives an activation energy of 140 cm^{-1} . On the other hand, the decrease of the 630-nm band intensity is probably due to the increasing tendency toward multiphonon relaxation to the ground electronic state of $KAu(CN)_2$ because the CN vibration energy is 2160 cm^{-1} .

Conclusions

The luminescence behavior of the layered compound $KAu(CN)_2$ can be described by a bonding model in which the Au–Au orbitals overlap. A plot of the energy of the high-energy emission band vs. R_{Au-Au}^{-3} confirms that Frenkel exciton behavior exists as in one-dimensional solids. Vibronic structure for the high-energy band is assigned to a CN symmetric stretch mode progression.

A low-energy emission band exists in pure $KAu(CN)_2$ that is assigned to a chemical trap. However, when $Au(CN)_2^-$ is doped into potassium cyanide crystals, the low-energy band does not appear but the high-energy band appears at 78 K with vibronic structure shifted slightly to lower energy compared with that of $KAu(CN)_2$. This implies that clusters of $Au(CN)_2^-$ exist in KCN without light-emitting traps.

Registry No. $KAu(CN)_2$, 13967-50-5.

- (17) Anpo, M.; Kubokawa, Y. *J. Phys. Chem.* **1984**, *88*, 5556.
 (18) Coluccia, S.; Tench, A. J. *J. Chem. Soc., Faraday Trans. 1* **1983**, *79*, 1881.

- (19) Kambli, U.; Gudel, H. U. *Inorg. Chem.* **1984**, *23*, 3479.

Contribution from the Lehrstuhl für Anorganische Chemie I, Ruhr-Universität, D-4630 Bochum, FRG, Fachbereich Chemie, Philipps-Universität, D-3550 Marburg, FRG, Anorganisch-Chemisches Institut der Universität, D-6900 Heidelberg, FRG, and Department of Chemistry, State University of Leiden, 2300 RA Leiden, The Netherlands

Variable-Temperature Single-Crystal Electron Spin Resonance Study and Crystal Structure of $[Cu(C_6H_{15}N_3)_2][Cu(CN)_3] \cdot 2H_2O$ at 110 and 293 K. Static and Dynamic Jahn–Teller Distortions in the CuN_6 Polyhedron

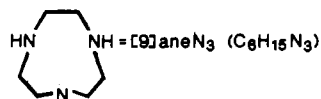
Phalguni Chaudhuri,^{1a} Karen Oder,^{1a} Karl Wiegardt,^{*1a} Johannes Weiss,^{1b} Jan Reedijk,^{1c} Winfried Hinrichs,^{1c} John Wood,^{*1c,d} Andrej Ozarowski,^{1e} Horst Stratemaier,^{1c} and Dirk Reinen^{*1e}

Received February 20, 1986

The reaction of $CuCl_2 \cdot 2H_2O$ in aqueous solution containing 1,4,7-triazacyclononane ($[9]aneN_3$, $C_6H_{15}N_3$) and KCN afforded blue crystals of $[Cu([9]aneN_3)_2][Cu(CN)_3] \cdot 2H_2O$, the crystal structure of which has been determined at 110 and 293 K. The complex crystallizes in the monoclinic crystal system, space group $P2_1/n$. Crystal data at 110 K and (in brackets) at 293 K: $a = 13.119$ (2) Å [13.061 (3) Å], $b = 12.116$ (2) Å [12.380 (3) Å], $c = 13.452$ (2) Å [13.503 (4) Å], $\beta = 93.90$ (2)° [93.06 (2)°] and $Z = 4$. The structures were refined to conventional R values of 0.024 [0.045] by using 2881 [3547] unique reflections. The compound consists of $[Cu([9]aneN_3)_2]^{2+}$ cations, $[Cu(CN)_3]^{2-}$ anions, and water of crystallization. The geometry of the CuN_6 core is a tetragonally elongated octahedron. At 110 K a maximum Jahn–Teller distortion is displayed with two long axial Cu–N bonds (2.305 (2) and 2.336 (2) Å) and four shorter equatorial Cu–N distances (average 2.062 Å), whereas at 293 K a dynamic component is obviously involved; the two axial Cu–N distances are at 2.222 (3) and 2.234 (3) Å and the average equatorial Cu–N distance is at 2.111 Å. The anion $[Cu(CN)_3]^{2-}$ is trigonal planar; the Cu–C and C–N bond lengths (average 1.934 and 1.135 Å, respectively) do not vary significantly between 110 and 293 K. Single-crystal and powder EPR spectra have been recorded at various temperatures (4.2–340 K), and a model for the dynamic averaging process within the CuN_6 polyhedra is proposed. An analysis of the thermal motion ellipsoids has been attempted with only limited success in order to further characterize the partial dynamic character of the CuN_6 core at 293 K.

Introduction

The small macrocyclic N donor 1,4,7-triazacyclononane ($[9]aneN_3$) is a strong ligand that forms very stable octahedral or distorted-octahedral bis complexes with many divalent and trivalent metal cations of the first transition-metal series.



A series of these complexes have been thoroughly studied by spectroscopy (electronic spectra, EPR spectra) and X-ray crystallography, i.e. bis complexes of Cr^{3+} , Mn^{2+} , Fe^{2+} , Fe^{3+} , Co^{2+} , Co^{3+} , Ni^{2+} , and Ni^{3+} .^{2,3,4,5,6,7,9,10,11} Their stability toward

- (1) (a) Ruhr-Universität Bochum; (b) Universität Heidelberg; (c) State University of Leiden; (d) Visiting professor from the Chemistry Department, University of Massachusetts, Amherst, MA; (e) Philipps-Universität.

- (2) Wiegardt, K.; Schmidt, W.; Herrmann, W.; Küppers, H. *J. Inorg. Chem.* **1983**, *22*, 2953–2956.
 (3) Boeyens, J. C. A.; Forbes, A. G. S.; Hancock, R. D.; Wiegardt, K. *Inorg. Chem.* **1985**, *24*, 2926–2931.
 (4) Küppers, H. J.; Neves, A.; Pomp, C.; Ventur, D.; Wiegardt, K.; Nuber, B.; Weiss, J. *Inorg. Chem.*, in press.
 (5) Koyama, H.; Yoshino, T. *Bull. Chem. Soc. Jpn.* **1972**, *45*, 481–484.
 (6) Mikami, W.; Kuroda, R.; Konno, M.; Saito, Y. *Acta Crystallogr., Sect. B: Struct. Crystallogr. Cryst. Chem.* **1977**, *B33*, 1485–1489.
 (7) Yang, R.; Zompa, L. J. *Inorg. Chem.* **1976**, *15*, 1499–1502.